

# Self-assembled complexes of multibranched gold nanoparticles with porphyrins used in photodynamic therapy

## Spectral and structural characterization

Juliana C. Araújo-Chaves<sup>1</sup>, Érica G. A. Miranda<sup>1</sup>, Aryane Tofanello, Carlos E. de Castro, Fernando C. Giacomelli, Alejandro Zúñiga and Iseli L. Nantes\*

**Abstract** — *The size and form of gold nanoparticles are crucial for the material properties. Particularly, anisotropic nanostructures are of particular interest because the capacity to enhance electromagnetic field upon irradiation for application in Surface Enhanced Raman Scattering spectroscopy and imaging. In the present study, biocompatible multibranched gold nanoparticles (MGNP) were synthesized by the one pot method using the piperazine moiety of HEPES buffer as reducing and stabilizing agent. The synthesis of MGNP was carried out at pH 3, 7 and 10 by using 0.2, 1.0, 2.5, 5.0 and 25.0 mM HEPES and phosphate buffer. The formation of stable MGNP in high yield was obtained using 2.5 mM HEPES buffer at pH values of 7.0 and 10.0 as evidenced by the deep blue color and the presence of red shifted resonance plasmon bands. The MGNP obtained in these conditions were used for association with cationic and anionic meso-tetrakis porphyrins, TMPyP (5, 10, 15, 20 tetrakis(1-methyl-4-pyridinio) porphyrin tetra(p-toluenesulfonate) and TPPS4 ((4, 4', 4'', 4''')-(porphyrine-5, 10, 15, 20 tetrayl) tetrakis benzenesulfonic acid. These porphyrins were the choice because the well-known application in photodynamic therapy (PDT). TMPyP and TPPS4 bound to the MGNPs as evidenced by changes of zeta potential ( $\zeta$ ). MGNP exhibited  $\zeta$  potential of -35 mV. The  $\zeta$  potential increased to -15 mV in the presence of TMPyP and decreased to -37 mV in the presence of TPPS4. Electronic absorption spectra analysis revealed that TMPyP redshifted the resonance plasmon band of MGNP suggesting the formation of elongated aggregates. TPPS4 did not promote changes in the plasmon resonance band of MGNP. Fluorescence spectroscopy analysis revealed changes in the fluorescence spectra of both MGNP and porphyrins. TMPyP exhibited a 50% quenched emission band. TPPS4 in homogeneous media when excited at 433 nm presented a fluorescence band peaking at 675 nm. The association with MGNP promoted a split of the TPPS4 fluorescence band with peaks at 643 and 707 nm suggestive of the conversion of the acidic porphyrin ( $H_2TPPS4$ ) to the desprotonated form TPPS4.*

**Keywords**— *multibranched gold nanoparticles, green synthesis, plasmonic band, HEPES buffer, zeta potential, fluorescence.*

From Universidade Federal do ABC, Santo André, SP, Brazil. <sup>1</sup>JCA-C and EGAM contributed equally for this paper; \*Corresponding author: Iseli L. Nantes:

## I. Introduction

Anisotropic gold nanoparticles are of great interest because their specific properties and applications which are shape- and size-dependent. The synthesis of these nanoparticles have motivated experimental progress in understanding the intrinsic shape-dependent properties of metal associated with the thermodynamic and kinetic parameters, type of reducing agent and buffer medium (1-3). These nanostructures have specific applications including nanoscale electronics, photovoltaic energy, biological markers, chemical sensing, and surface enhanced Raman scattering, among others (1, 4, 5). Specifically, noble metal nanoparticles exhibit a surface-enhanced Raman scattering (SERS) activity in which the scattering cross-sections are largely enhanced for molecules adsorbed thereon (6) and this SERS property is highly sensitive to the shape and size of nanoparticles (7). Another motivator factor for the study of these structures is the contribution for elucidation of the particle growth mechanisms, which in turn contribute for the prediction and systematic manipulation of the final nanostructure (8). Finally, these new particles provide new template systems for the further generation of different structures and applications (9).

Different features of anisotropic gold nanoparticles have been produced such as nanorods, nanoprisms, nanocubes, nanocages, nanoshells and the multibranched NPs featured as nanostars, nanoflowers, and the sea urchin-like nanocrystals. These nanostructures are attracting interest, due to its wide range of applications (2). The surface plasmon resonance (SPR) of multibranched gold nanoparticles (MGNPs) are tuned to the near-infrared (NIR) region (10-13). This spectroscopic characteristic is important because it allows applications for photodynamic therapy that requires efficient tissue penetration of light (13, 14) and for optical bioimaging techniques (13, 15).

HEPES (2-[4-(2-hydroxyethyl)piperazinyl]ethanesulfonic acid) is a pH buffer (Goods buffer) widely used in laboratories of analytical, inorganic, physical, biological, biochemical and also in tissue culture due to its mild pKa value (7.55), high solubility, complexation and minimalist with metal ions (1). Good's buffers, such as Tris and HEPES, are not inert as was previously believed. They are able to generate N-oxides in the presence of molecular oxygen (4). HEPES buffer has been used for the synthesis of a one step MGNPs. In the synthesis of MGNPs, HEPES acts as reducing

and growth-directing agent because the piperazine moiety is able to generate nitrogen-centered free radicals, which can reduce gold ions ( $\text{AuCl}_4^-$ ). Another interesting characteristic of metallic nanoparticles is the capacity to modify the properties molecules associated to their surface (16-17). Therefore, in the present study, we characterized the binding capacity of two *meso*-tetrakis porphyrins, the cationic *meso*-tetrakis porphyrins, TMPyP (5, 10, 15, 20 tetrakis(1-methyl-4-pyridinio) porphyrin tetra(p-toluenesulfonate) and the anionic TPPS4 ((4, 4', 4'', 4''')-(porphyrine-5, 10, 15, 20 tetrayl) tetrakis benzenesulfonic acid free base) to sea urchin-like MGNPs produced by using HEPES as reducing and stabilizing agents (7).

## II. Materials and Methods

### A. Chemicals

All chemicals were purchased from Sigma-Aldrich Corp. (St. Louis, MO, USA). The TMPyP stock solution concentration was checked using the absorption coefficient  $\epsilon_{423\text{nm}} = 2.26 \times 10^5 \text{ M}^{-1} \text{ cm}^{-1}$  and TPPS4 at  $\epsilon_{412\text{nm}} = 5.30 \times 10^5 \text{ M}^{-1} \text{ cm}^{-1}$ . All aqueous suspensions and solutions were prepared with deionized water (mixed bed of ion exchanger, Millipore®), and the pH was measured using a combined glass electrode (Orion Glass pH SURE-FLOW™). The reference electrode (ROSS™, model 8102) was filled with Orion Filling Solutions (ROSS™). The pH meter was calibrated using METREPAK pHydrion standard buffer solutions (Brooklyn, NY) Chemicals.

GNPs were synthesized at pH 3, 7 and 10 by using 0.2, 1.0, 2.5, 5.0 and 25.0 mM HEPES and phosphate buffer and 450  $\mu\text{M}$   $\text{HAuCl}_4$  salt. The growth reaction occurred fill seconds after the dropwise addition of  $\text{HAuCl}_4$  salt in presence of HEPES buffer, which was used as reducing and stabilizing agent (4). The syntheses were carried out at room temperature and the size and nanostructuring of NP were dependents of HEPES buffer concentration (figure 1).

### B. Electronic absorption spectra measurements

The electronic absorption spectra of porphyrins were measured by using a Varian Cary 50, Varian Inc. (CA, United States) spectrometer. The spectral resolution for wavelength scan was 0.5 nm. The optical path length was 1 cm for the porphyrin and MGNP spectra measurements.

### C. CD and MCD measurements

The CD and MCD measurements were carried out in a Jasco J-720 spectropolarimeter (Easton, MD) using quartz cuvettes with a 0.1 cm optical path; band width, 1.0 nm; scanning speed, 100 nm/min; response, 0.5 s; and accumulations, 4.0. For the MCD measurements, the magnetic field was 995 mT.



Figure 1. Digital snapshot of GNPs synthesized using HEPES buffer (inset above) as reducing and stabilizing agent, from the left to the right, in the following conditions, respectively: 2.5 mM HEPES at pH 7.0; 2.5 mM HEPES at pH 7.0 in the presence of PEG; 2.5 mM HEPES at pH 7.0 and PEG added immediately after the synthesis, 5.0 mM HEPES pH 7.0, 2.5 mM HEPES at pH 10.0 and 25 mM HEPES pH 10.0. Phosphate buffer were present in all conditions in the same concentration of HEPES and the synthesis was carried out at room temperature.

### D. Determination of zeta potential ( $\zeta$ )

The measurements of Zeta potential were carried out in a Zetasizer Nano ZS, Malvern Instruments, Ltd. (London, UK), at the temperature of 25°C. The zeta potential,  $\zeta$ , is determined by the electrophoretic mobility,  $\mu_e$  by the application of the Henry equation and calculated by using the Smoluchowski approximation. The  $\zeta$  values are the average of 10 independent measurements that were calculated using a mono-modal model and time measurement was determined by the instrument. For each zeta potential measurements, the samples were previously equilibrated for 2 min at 25°C.

### E. Scanning Electron Microscopy (SEM)

The samples (deposited onto a carbon ribbon) were carried out using a scanning electron microscopy (FEG-SEM) field emission by scanning of ultra-high vacuum FESEM JMS-6701F, JEOL (Tokyo, Japan) operated at an 5 kV acceleration voltage and 60,000 and 370,000 X magnification.

### F. Fluorescence spectra measurements

The fluorescence spectra of porphyrins were measured by using a Cary Eclipse, Varian (CA, United States) spectrometer. The spectral resolution for wavelength scan was 0.5 nm. The optical path length was 1 cm for the porphyrin and MGNP spectra measurements.

### G. Dynamic Light Scattering (DLS)

DLS measurements were performed using an ALV/CGS-3 compact goniometer system consisting of a 22 mW HeNe linearly polarized laser operating at a wavelength of 633 nm, an ALV 7004 digital correlator, and a pair of avalanche photodiodes operating in the pseudo-cross-correlation mode. The samples were placed in 10 mm diameter glass cells and maintained at a constant temperature of  $25 \pm 1$  °C. The autocorrelation functions reported are based on three independent runs of 60 s counting time. The data were collected and further averaged by using the ALV Correlator Control software.

## H. FTIR analysis

The FTIR spectra were collected at resolution of  $4\text{ cm}^{-1}$  in the transmission mode ( $4000 - 400\text{ cm}^{-1}$ ) using a Shimadzu FTIR spectrophotometer (FTIR 8400).

## III. Results

Multibranched gold nanoparticles (MGNP) were synthesized by using the piperazine moiety of HEPES buffer as reducing and stabilizing agent (4). The synthesis of MGNP was carried out at pH 3, 7 and 10 by using 0.2, 1.0, 2.5, 5.0 and 25.0 mM HEPES and phosphate buffer. The best condition for the formation of stable MGNP (blue) in high yield was obtained using 2.5 mM HEPES buffer at pH values of 7.0 and 10.0 as evidenced by the deep blue color (Figure 1, the first and fifth tubes, from left to right, respectively). The deep blue color is indicative of the formation of MGNP. Differently of spherical GNP colloidal suspensions that presents the typical red color, a blue color is observed for the colloidal solution of the MGNPs. Addition of polyethyleneglycol in 2.5 mM HEPES/phosphate buffer, pH 7.0, before addition of  $\text{HAuCl}_4$  solution prevented the growing of the tips and the synthesis resulted in a purple colloidal suspension (Fig. 1, second tube, from left to right). Addition of PEG after MGNP synthesis obtained by using 2.5 mM HEPES, pH 7.0 did not affect the deep blue color of the suspension (Fig. 1, third tube from left to right). Also, PEG addition after MGNP synthesis prevented gradual change of the deep blue to violet color that was observed for the samples stored for 24 h, at room temperature and unprotected of light. The formation of MGNPs was reinforced by the analysis of the surface plasmon resonance (SPR) band of the deep blue suspension obtained using 2.5 mM HEPES, pH 7.0, in comparison with the SPR band presented by the red suspension obtained using 5.0 mM HEPES at the same pH value (Fig. 2). The SPR bands of the deep blue and red color suspensions peak at 632 and 537 nm, respectively (Fig. 2). The SPR band of MGNPs can peak at the range from 650 to 700 nm, depending on the conditions of synthesis. The extension of the red shift is dependent the average size of MGNPs (4). The broad SPR band exhibited by the deep blue colloidal suspension was consistent with the presence of MGNPs in this sample. The branched GNPs are generally not highly monodisperse. The three-tipped nanoparticle is the more common shape found for MGNPs. These MGNPs exhibit LSPR at 700 nm and 540 nm. Accordingly to discrete dipole approximation (DDA) calculations considering a model structure, the band at 700 nm is the contribution of a dipole resonance in the plane of the NP, and the 540 nm the contribution of a quadrupole resonance out of the plane of the NP. Several authors have been characterized, (14, 17-20) that, accordingly simplified 2D modelling, SPR peak wavelength is correlated with the branching and the peak intensity depends on the polarization angle. Consistently, the decomposition of the spectrum of the deep blue sample resulted in the contribution of two bands peaking at 534 and 674 nm (red and blue lines of Fig. 2 inset, respectively).

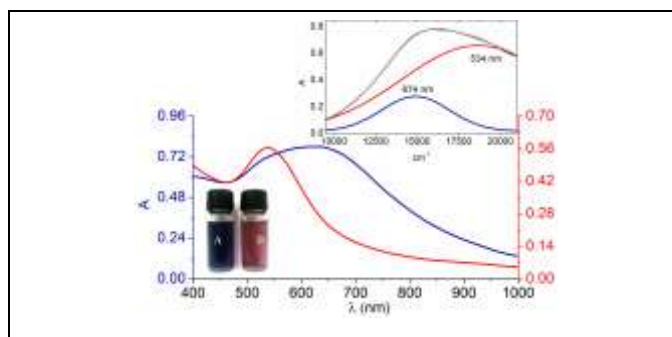


Figure 2. UV-visible spectra of branched GNPs obtained using two different concentrations of HEPES and different conditions of storage. The royal line corresponds to the spectrum obtained immediately after the synthesis using 2.5 mM HEPES buffer, pH 7.0. The violet and blue lines correspond to two aliquots of that NP sample stored unprotected and protected of light, respectively. The red line corresponds to the synthesis using 5 mM HEPES buffer at pH 7.0.

The presence of MGNPs in the blue sample was reinforced by DLS measurements. For the deep blue sample it was obtained a hydrodynamic radius (RH) of 63 nm and polydispersity ( $\mu_2/\Gamma_2$ ) = 0.45 and for the red sample the value of RH was of 15 nm and  $\mu_2/\Gamma_2$  = 0.48. Scanning electronic microscopy images of the deep blue color colloidal suspension revealed nanocrystals with multiple branches with a sea urchin-like feature. The large number of branches are projected from the whole particle surface. The sea urchin-like feature differs of others previously characterized nanostructures that were obtained using HEPES as reducing and stabilizing agent that more frequently formed nanostars structures. The asymmetry of the MGNP obtained with 2.5 mM HEPES, pH 7.0 is corroborated by the chiroptical properties evidenced by the circular and magnetic circular dichroism of these nanostructures showed in Fig. 3 C and D, respectively. The GNPs synthesized using 2.5 and 5.0 mM HEPES, pH 7.0 were associated with cationic and anionic *meso*-tetrakis porphyrins, TMPyP (5, 10, 15, 20 tetrakis(1-metyl-4-pyridinio) porphyrin tetra(p-toluenesulfonate) and TPPS4 ((4, 4', 4'', 4''')-(porphyrine-5, 10, 15, 20 tetrayl) tetrakis benzenesulfonic acid. These porphyrins were the choice because the well-known application in photodynamic therapy (PDT) (21). The association of the porphyrins with GNPs was evidenced by changes of zeta potential ( $\zeta$ ). MGNP (blue colloidal suspension) exhibited  $\zeta$  potential of -35 mV. The  $\zeta$  potential increased to -15 mV in the presence of the cationic porphyrin TMPyP and decreased to -37 mV in the presence of the anionic TPPS4 (Table I). Interestingly, TMPyP promoted a more significant decrease of the  $\zeta$  potential for the GMNPs obtained with 2.5 mM HEPES than for the GNPs obtained with 5.0 mM HEPES (red colloidal suspension). This result is consistent with a drastic increase of the surface area that is expected for the multibranched particles. Electronic absorption spectra analysis revealed that TMPyP redshifted the resonance plasmon band of MGNP suggesting the formation of elongated aggregates in a time-dependent manner. However, TPPS4 did not change the SPR of MGNPs (Fig. 4, gray line) and the resulting spectrum was the sum of the contribution of MGNPs and TPPS4.

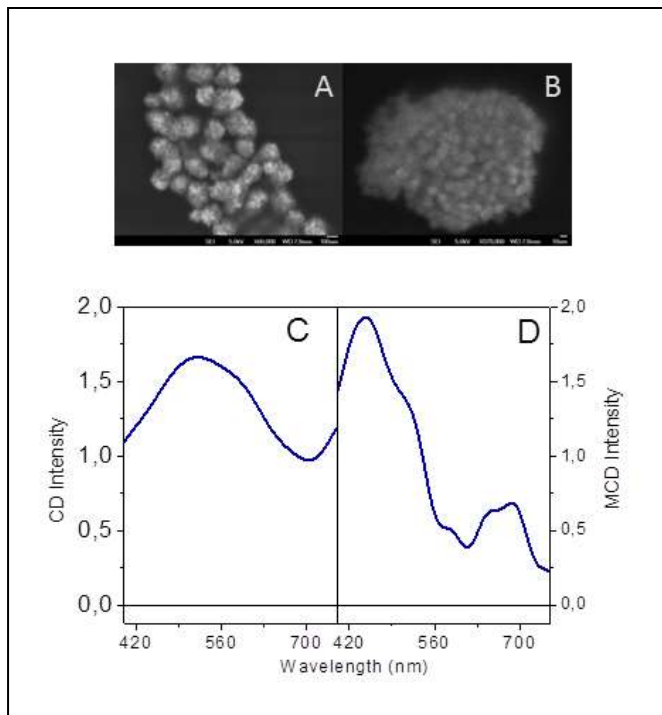


Figure 3. Anisotropy of MGNPs. Field-emission scanning electron microscopy (FEG-SEM) images of MGNPs synthesized using 2.5 mM HEPES at pH 7.0 A) 60,000 X magnified and B) 370,000 X magnified; circular C) and magnetic circular dichroism D) of MGNPs.

TABLE I. ZETA POTENTIAL ( $\zeta$ ) OF GNPs IN THE ABSENCE AND IN THE PRESENCE OF PORPHYRINS

[HEPES] (mM) <sup>a</sup>	Nanostructure		
	GNP (mV)	GNP + TMPyP (mV)	GNP + TPPS4 (mV)
2.5	- 34.8 +/- 1	- 15.1 +/- 1	- 37.1 +/- 1
5.0	- 15.2 +/- 1	- 13.2 +/- 1	- 18.6 +/- 2

<sup>a</sup> pH = 7.0

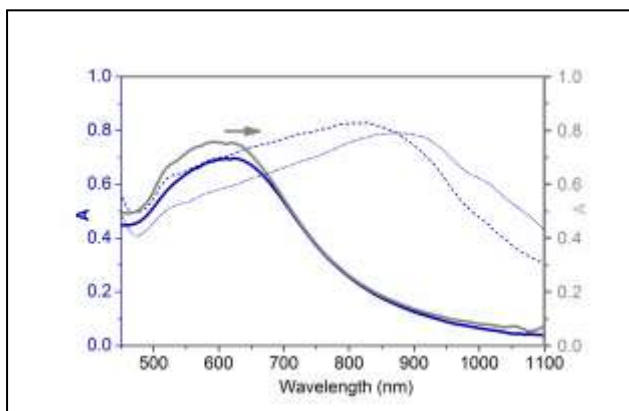


Figure 4. Effect of porphyrins on the MGNPs' SPR. Royal solid line represent the SPR of MGNP obtained with 2.5 mM HEPES, pH 7.0. The dash and dotted royal lines, the SPR of MGNPs immediately and 1 min after 10  $\mu$ M TMPyP addition and the gray line the SPR of MGNPs after addition of 10  $\mu$ M TPPS4.

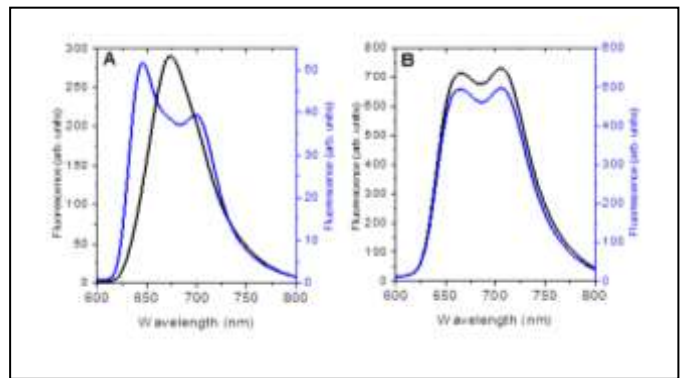


Figure 5. Effect of MGNPs on the fluorescence spectra of TPPS4 and TMPyP. A) Black line corresponds to the spectrum of TPPS4 (slit 5 nm) and blue line corresponds to the spectrum of the porphyrin associated to MGNPs (slit 10 nm). B) Black line corresponds to the spectrum of TMPyP and blue line corresponds to the spectrum of the porphyrin associated to MGNP (both slit 10 nm).

Fluorescence spectroscopy analysis revealed changes in the fluorescence spectra of both MGNP and porphyrins. TMPyP exhibited a 50% quenched emission band. TPPS4 in homogeneous media when excited at 433 nm presented a fluorescence band peaking at 675 nm. The association with MGNP promoted a split of the TPPS4 fluorescence band with peaks at 643 and 707 nm suggestive of the conversion of the acidic porphyrin ( $H_2$ TPPS4) to the desprotonated form TPPS4.

## iv. Conclusions

HEPES buffer acts as reducing and stabilizing agent for a one pot synthesis of anisotropic gold nanocrystals at room temperature. The feature of gold nanocrystals was modulated by the pH and buffer concentration. Deep blue colloidal suspensions were observed only at HEPES concentration of 2.5 mM. Acidic pH values were unfavorable for the MGNP synthesis. The MGNPs synthesized according to this protocol featured as sea urchin-like particles and exhibited CD and MCD signals. The MGNPs were able to bind the cationic and anionic porphyrins, TMPyP and TPPS4 and changed the fluorescence spectrum of the latter to the unprotonated form. TMPyP promoted significant redshift of the MGNP SPR to the near infrared spectral region and constituted a promising system to be applied in photodynamic therapy.

## Acknowledgment

The authors thank to the financial support of Brazilian agencies: FAPESP (2012/07456-7), CNPq and CAPES. The present study had also financial support of UFABC (NBB – Núcleo de Bioquímica e Biotecnologia). The authors thank also to Central Experimental Multiusuários of UFABC for the access to facilities and to David da Mata Lopes for the technical assistance. J.C.A-C is post-doctoral fellow of FAPESP (2012/08322-4).

## References

- [1] A. Habib, and M. Tabata, "Oxidative DNA damage induced by HEPES (2-[4-(2-hydroxyethyl)-1-piperazinyl]ethanesulfonic acid) buffer in the presence of Au(III)," *J. Inorg. Biochem.*, vol. 98, pp. 1696-1702, November 2004.
- [2] R. Chen, J. Wu, H. Li, G. Cheng, Z. Lu, and C.-M. Che, "Fabrication of gold nanoparticles with different morphologies in HEPES buffer," *Rare Metals*, vol. 29, pp. 180-186, April 2010.
- [3] A.R. Tao, S. Habas, and P.D. Yang, "Shape control of colloidal metal nanocrystals" *Small*, vol. 4, pp. 310-325, March 2008.
- [4] G. Maiorano, L. Rizzello, M. A. Malvindi, S. S. Shankar, L. Martiradonna, A. Falqui, R. Cingolani, and P. P. Pompa, "Monodispersed and size-controlled multibranching gold nanoparticles with nanoscale tuning of surface morphology," *Nanoscale*, vol. 3, pp. 2227-2232, April 2011.
- [5] Y. Xia, Y. Xiong, B. Lim, S. E. Skrabalak, "Shape-Controlled Synthesis of Metal Nanocrystals: Simple Chemistry Meets Complex Physics?," *Angew Chem Int Ed.*, vol. 48, pp. 60-103, January 2009
- [6] B. R. Danger, D. Fan, J. P. Vivek, and I. J. Burgess, "Electrochemical Studies of Capping Agent Adsorption Provide Insight into the Formation of Anisotropic Gold Nanocrystals," *ACS Nano*, vol. 6, pp. 11018-11026, November 2012.
- [7] S.R. Saptarshi, A. Duschl, and A.L. Lopata, "Interaction of nanoparticles with proteins: relation to bio-reactivity of the nanoparticle," *J. of Nanobiotechnology*, vol. 11, pp.26-38, July 2013.
- [8] G. H. Jeong, Y. W. Lee, M. Kim, S. W. Han, "High-yield synthesis of multi-branched gold nanoparticles and their surface-enhanced Raman scattering properties," *Journal of Colloid and Interface Science*, vol. 329, pp. 97-102, January 2009.
- [9] K. De Wael, H. Buschop, H. A. Heering, L. De Smet, J. V. Beeumen, B. Devreese, A. Adriaens, "Electrochemical determination of hydrogen peroxide using Rhodobacter capsulatus cytochrome c peroxidase at a gold electrode," *Microchim Acta*, vol. 162, pp. 65-71, January 2008.
- [10] R. Aroca, *Surface enhanced vibrational spectroscopy*, Hoboken, NJ: Wiley, 2006.
- [11] S.-M. Lee, Y.-W. Jun, S.-N. Cho, J. Cheon., "Single-crystalline star-shaped nanocrystals and their evolution: Programming the geometry of nano-building blocks," *J. of the Am.n Chem. Soc.*, vol. 124, pp. 11244-11245, September 2002.
- [12] N. Ortiz, and S.E. Skrabalak, "Controlling the Growth Kinetics of Nanocrystals via Galvanic Replacement: Synthesis of Au Tetrapods and Star-Shaped Decahedra," *Crystal Growth & Design*, vol. 11, pp. 3545-3550, August 2011.
- [13] X. Zou, E. Ying, and S. Dong, "Seed-mediated synthesis of branched gold nanoparticles with the assistance of citrate and their surface-enhanced Raman scattering properties," *Nanotechnology*, vol. 17, pp. 4758-4764, September 2006.
- [14] E. Hao, R. C. Bailey, G. C. Schatz, J. T. Hupp, and S. Li., "Synthesis and optical properties of "branched" gold nanocrystals," *Nano Letters*, vol. 4, p p. 327-330, September 2004.
- [15] X.H. Huang, S. Neretina, and M.A. El-Sayed, "Gold Nanorods: From Synthesis and Properties to Biological and Biomedical Applications," *Advanced Materials*, vol. 21, pp. 4880-4910, December 2009.
- [16] Zhang, J.Z., "Biomedical Applications of Shape-Controlled Plasmonic Nanostructures: A Case Study of Hollow Gold Nanospheres for Photothermal Ablation Therapy of Cancer," *Journal of Physical Chemistry Letters*, vol. 1, pp. 686-695, January 2010.
- [17] S. Trigari, A. Rindi, G. Margheri, S. Sottini, G. Dellepiane, and E. Giorgetti, "Synthesis and modelling of gold nanostars with tunable morphology and extinction spectrum," *Journal of Materials Chemistry*, vol. 21, pp. 6531-6540, March 2011.
- [18] H. Yuan, C. G. Khoury, H. Hwang, C. M. Wilson, G. A. Grant, and T. Vo-Dinh, "Gold nanostars: surfactant-free synthesis, 3D modelling, and two-photon photoluminescence imaging," *Nanotechnology*, vol. 23, February 2012.
- [19] J. Xie, Q. Zhang, J. Y. Lee, D. I. C. Wang, "The Synthesis of SERS-Active Gold Nanoflower Tags for In Vivo Applications," *ACS Nano*, vol. 2, pp. 2473-2480, November 2008.
- [20] X. Huang, X. Qi, Y. Huang, S. Li, C. Xue, C. L. Gan, F. Boey, and H. Zhang "Photochemically Controlled Synthesis of Anisotropic Au Nanostructures: Platelet-like Au Nanorods and Six-Star Au Nanoparticles," *ACS Nano*, vol. 4, pp. 6196-6202, October 2010.
- [21] C. Kawai, J. C. Araújo-Chaves, T. Magrini, C. O. C. C. Sanches, S. M. S. Pinto, H. Martinho, N. Daghestanli, and I. L. Nantes, "Photodamage in a Mitochondrial Membrane Model Modulated by the Topology of Cationic and Anionic Meso-Tetrakis Porphyrin Free Bases," *Photochem. and Photobiol.*, vol. 90, pp. 596-608, May/June 2014.

### About Authors:



Juliana C. Araujo-Chaves is Postdoc in UFABC under the supervision of Professor Iseli L. Nantes. Her research interest focuses on porphyrins, membranes, and the synthesis of GNP for application in PDT.



Erica G. A. Miranda is PhD student under the guidance of Professor Iseli L. Nantes. Her research interest focuses on the photochemical synthesis of gold and silver nanoparticles using dyes.



Aryane Tofanello is PhD student under the guidance of Professor Iseli L. Nantes. Her research interest focuses on the synthesis of gold nanoparticles with thiol-containing peptides.



Carlos E. de Castro is Master's student working under the supervision of Professor Fernando Carlos Giacomelli. His investigations are focused on polymer colloids.



Fernando C. Giacomelli is Associate Professor in the Universidade Federal do ABC - UFABC (Brazil). His main research area is focused on the characterization of complex polymer assemblies.



Alejandro Zúñiga received his PhD in Materials Science and Engineering from the University of California, Davis. His research interests include nanostructured, amorphous materials and electron microscopy.



Iseli L. Nantes is full professor of Bioenergetics in Universidade Federal do ABC, Brazil. She coordinates projects focused on hemeproteins and porphyrins associated to membranes and nanoparticles.